



*Supplement of*

**Marine anoxia initiates giant sulfur-oxidizing bacterial mat proliferation and associated changes in benthic nitrogen, sulfur, and iron cycling in the Santa Barbara Basin, California Borderland**

David J. Yousavich et al.

*Correspondence to:* David J. Yousavich (yousavdj@ucla.edu) and Tina Treude (ttreude@g.ucla.edu)

The copyright of individual parts of the supplement might differ from the article licence.

**Table S1:** Porewater nitrite concentrations taken from sediment cores at SDRO and SDT3-A. Nitrite was below detection in sediment cores for all other stations.

Sediment Depth (cm)	SDRO [NO <sub>2</sub> <sup>-</sup> ] (μmol L <sup>-1</sup> )	SDT3-A [NO <sub>2</sub> <sup>-</sup> ] (μmol L <sup>-1</sup> )
-1	1.1	0.0
0.5	36.6	5.2
1.5	1.4	1.7
2.5	1.1	0.7
3.5	1.1	0.0
4.5	1.2	0.0
5.5	0.0	0.0
6.5	6.1	0.0
7.5	4.3	0.0
8.5	0.0	0.0
9.5	0.0	0.0
10.5	0.0	0.0
11	0.0	
13	0.0	
15	0.0	0.0
17	0.0	0.0
19		0.0

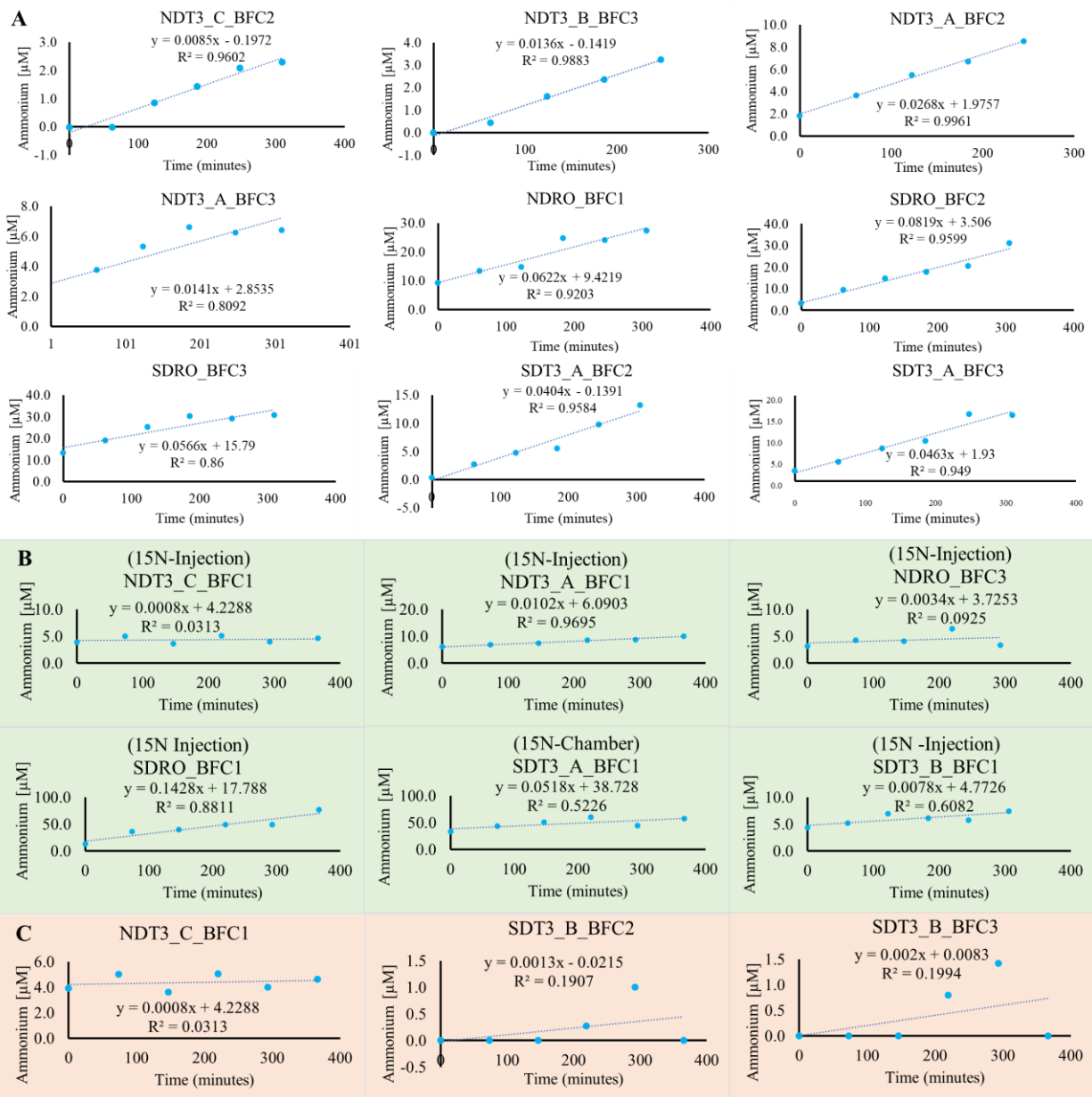


**Figure S1:** A) Ammonium concentration changes over time from benthic flux chamber (BFC1, BFC2, BFC3) incubations. B) Ammonium concentration changes over time from <sup>15</sup>N-Nitrate benthic flux chamber incubations. Note these chambers were not used to calculate benthic fluxes. C) Ammonium concentration changes over time from benthic flux chamber incubations where there was no calculatable flux. No data are shown from chambers if there was a mechanical failure with the deployment or ammonium concentrations were all below detection. For station abbreviation definitions please refer to the main manuscript.

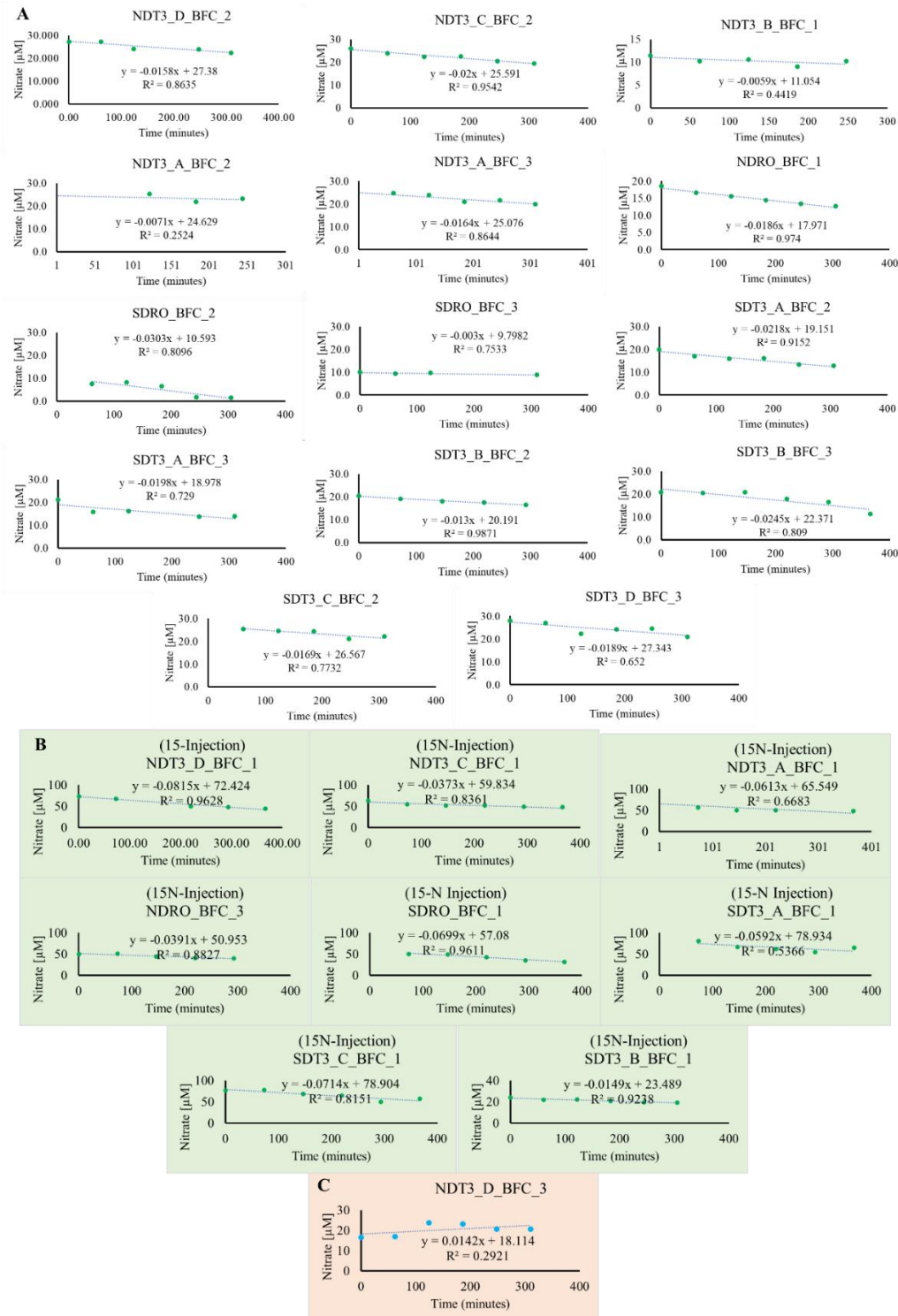


**Figure S2:** Nitrate concentration changes over time from benthic flux chamber (BFC1, BFC2, BFC3) incubations. B) Nitrate concentration changes over time from <sup>15</sup>N-Nitrate benthic flux chamber incubations. Note these chambers were not used to calculate benthic fluxes. C) Nitrate concentration changes over time from benthic flux chamber incubations where there was no calculatable flux. No data are shown from chambers if there was a mechanical failure with the deployment. For station abbreviation definitions please refer to the main manuscript.

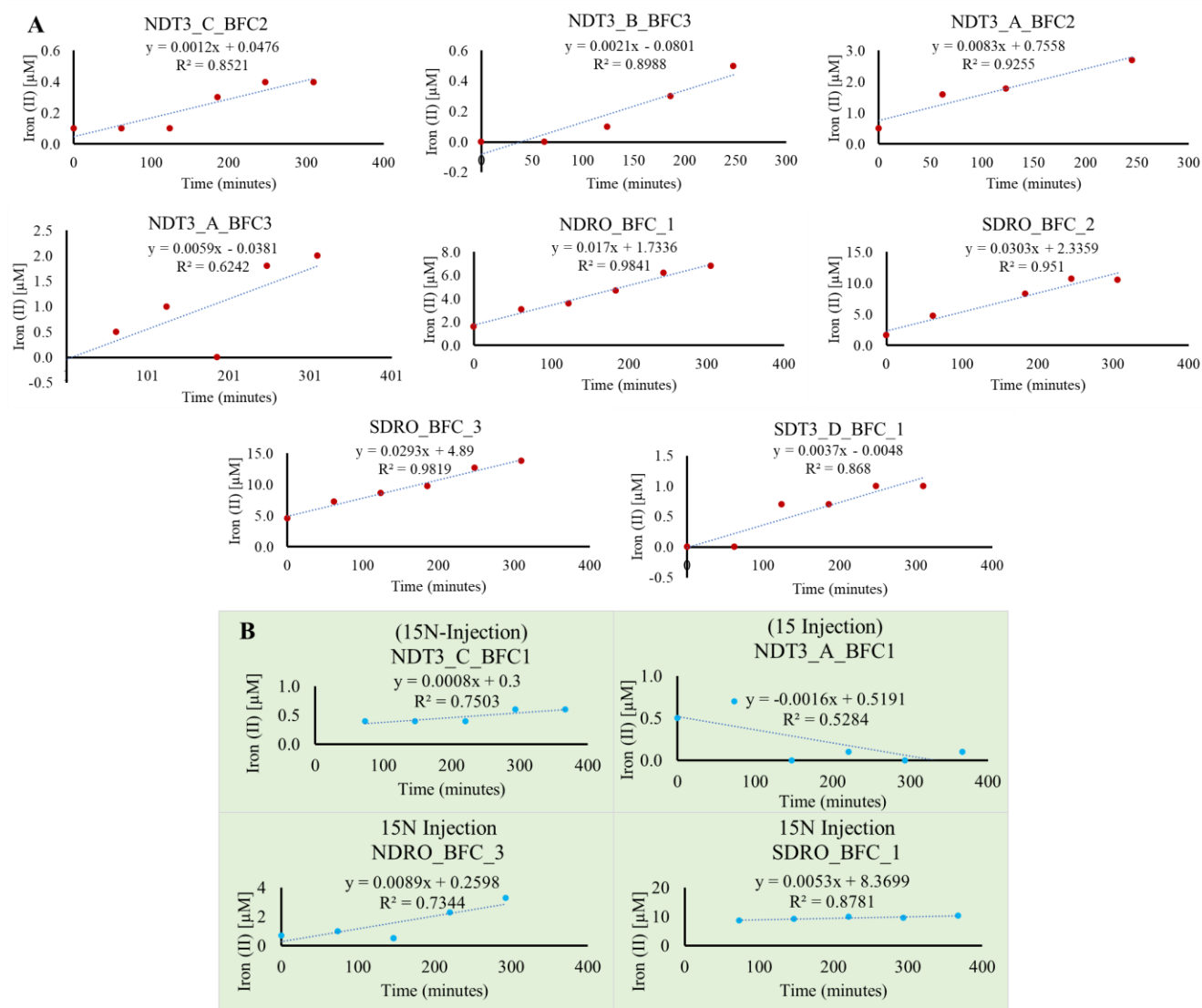


**Figure S3:** Iron (II) concentration changes over time from benthic flux chamber (BFC1, BFC2, BFC3) incubations. B) Iron (II) concentration changes over time from  $^{15}\text{N}$ -Nitrate benthic flux chamber incubations. Note these chambers were not used to calculate benthic fluxes. No data are shown from chambers if there was a mechanical failure with the deployment or concentrations were all below detection. For station abbreviation definitions please refer to the main manuscript.

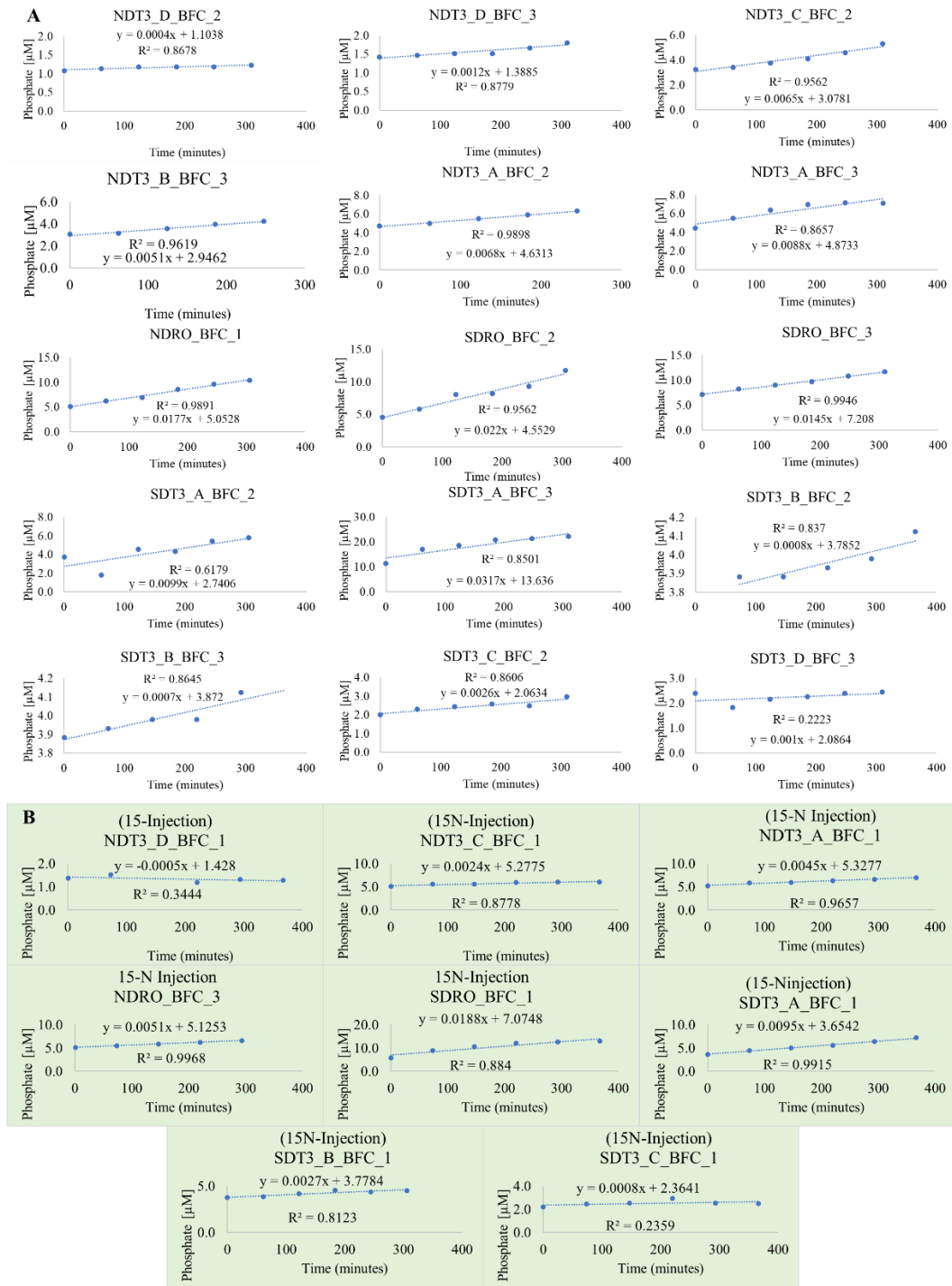


**Figure S4:** Phosphate concentration changes over time from benthic flux chamber (BFC1, BFC2, BFC3) incubations. B) Phosphate concentration changes over time from <sup>15</sup>N-Nitrate benthic flux chamber incubations. Note these chambers were not used to calculate benthic fluxes. No data are shown from chambers if there was a mechanical failure with the deployment or concentrations were all below detection. For station abbreviation definitions please refer to the main manuscript.

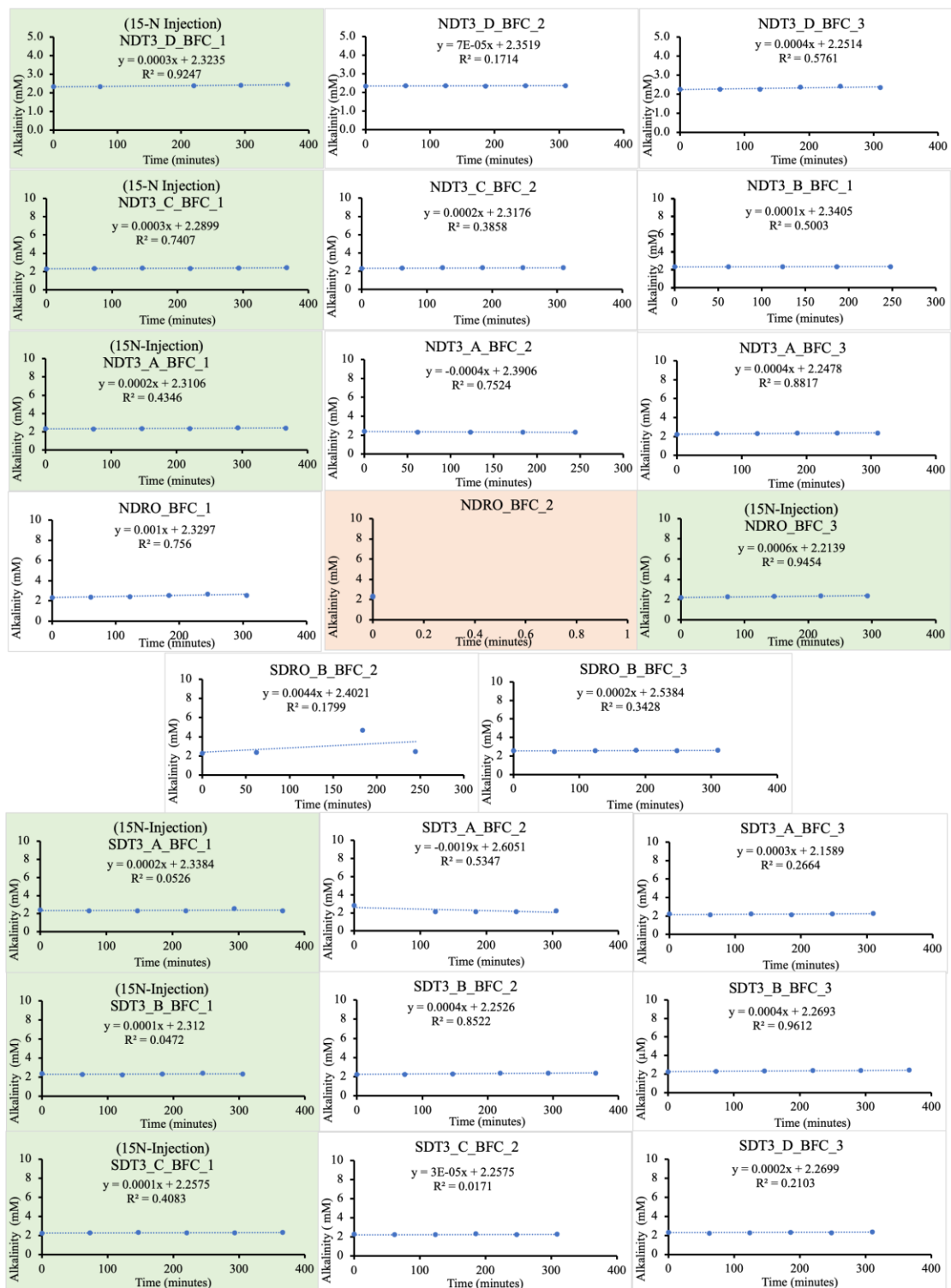


**Figure S5:** Total Alkalinity changes over time from benthic flux chamber (BFC1, BFC2, BFC3) incubations. No data are shown from chambers if there was a mechanical failure with the deployment or concentrations were all below detection. For station abbreviation definitions please refer to the main manuscript.

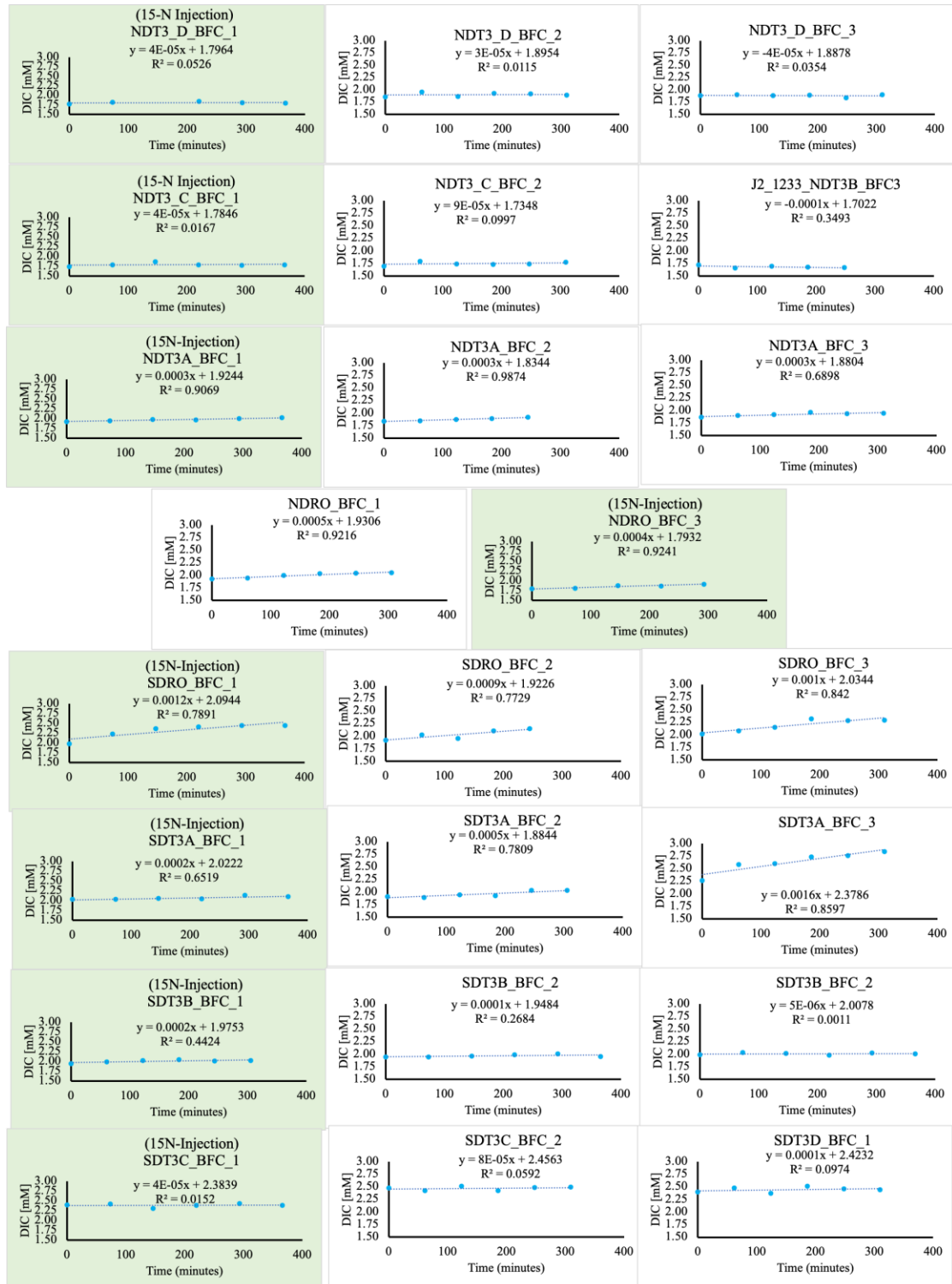


**Figure S6:** Dissolved Inorganic Carbon (DIC) changes over time from benthic flux chamber (BFC1, BFC2, BFC3) incubations. No data are shown from chambers if there was a mechanical failure with the deployment or concentrations were all below detection. For station abbreviation definitions please refer to the main manuscript.



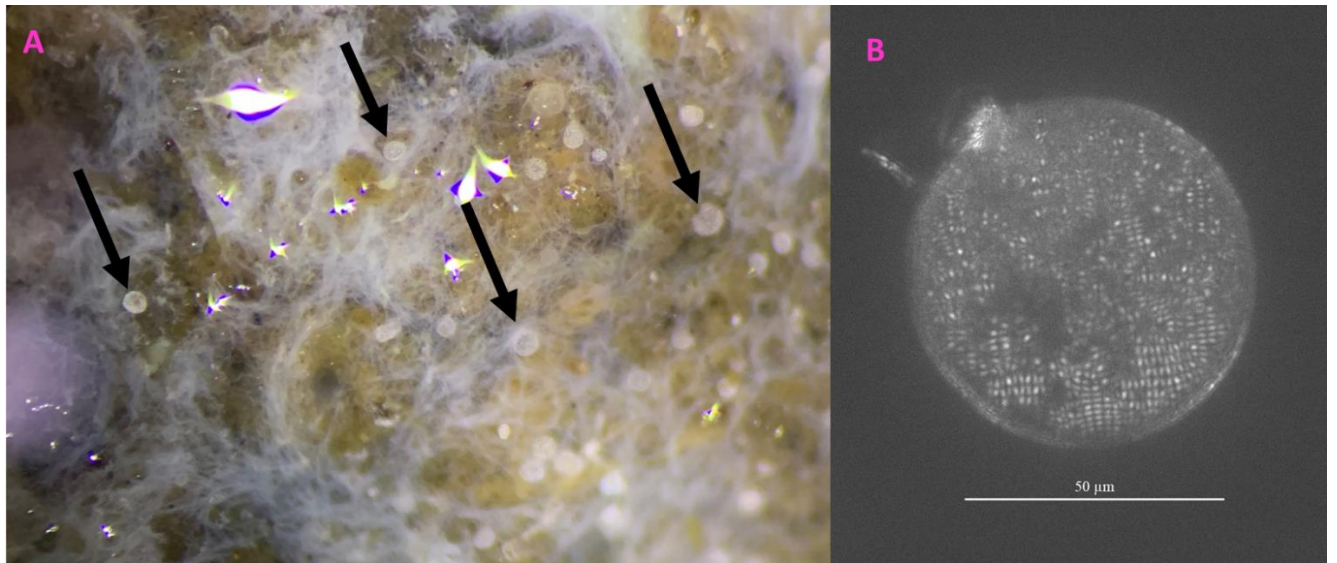


**Figure S7.** A) Photograph of spherical sulfur bacteria (nicknamed 'ghost balls') within a mat of filamentous sulfur bacteria as seen through a dissection microscope. Black arrows point to a few of the ghost balls. The size of the ghost ball radius ranges between 24.0 – 49.8  $\mu\text{m}$  ( $n = 8$ ). B) Light Microscopy image of representative ghost ball with a scale bar. Ghost Balls were sampled from the 0-1 cm section of a core collected from station NDRO.